Isotopic Constraints on Biogeochemical Cycling of Copper in the Ocean

Shotaro Takano[1*], Masaharu Tanimizu[2], Takafumi Hirata[3], and Yoshiki Sohrin[1]

[1]*Institute for Chemical Research, Kyoto University, Uji, Kyoto 611-0011, Japan*

[2]*Kochi Institute for Core Sample Research, Japan Agency for Marine-Earth Science and Technology, 200 Monobe Otsu, Nankoku 783-8502, Japan*

[3]*Laboratory for Planetary Sciences, Division of Earth and Planetary Sciences, Kyoto University, Kitashirakawa Oiwake-cho, Kyoto 606-8502, Japan*

[*]**Corresponding author.** E-mail: shotaro@inter3.kuicr.kyoto-u.ac.jp Tel: +81 774 38 3098. Fax: +81 774 38 3099

Trace elements and their isotopes are being actively studied as powerful tracers in the modern ocean and as proxies for the palaeocean. Although distributions and fractionations have been reported for stable isotopes of dissolved Fe, Cu, Zn, and Cd in the ocean, the data remain limited and only preliminary explanations have been given. Copper is of great interest because it is either essential or toxic to organisms and because its distribution reflects both biological recycling and scavenging. Here, we present new data of isotopic compositions of dissolved Cu (δ^{65}Cu) in seawater and rainwater. The Cu isotopic composition in surface seawater is explained by the mixing of rain, river, and deep water. In deep seawater, δ^{65}Cu becomes heavier along oceanic circulation because of preferential scavenging of the lighter isotope (^{63}Cu). Additionally, we constrain the marine biogeochemical cycling of Cu using a new box model based on Cu concentration and δ^{65}Cu.

Copper plays an important role as a micronutrient for organisms in the ocean, but high concentrations of the free Cu^{2+} ion are toxic[1]. Dissolved Cu has concentrations of 0.5−6 nmol kg^{-1} in seawater and mostly complexes with organic ligands, which results in very low concentrations (fmol kg^{-1} to pmol kg^{-1}) of the free Cu^{2+} ion[2].

Vertical distributions of dissolved Cu are of the nutrient-scavenging hybrid type[3]. Generally, the concentrations of nutrient-type trace metals (e.g., Zn, Ni, and Cd) are low in the surface layer of the ocean because of biological uptake. However, the concentrations increase with depth, showing a mid-depth maximum because of remineralisation from settling particles. By contrast, the concentration of dissolved Cu gradually increases with depth towards the bottom. Such distributions have been interpreted to be caused by a combination of scavenging throughout the water column and a supply from the uppermost layer of benthic sediments, where scavenged Cu is recycled to overlying seawater via early diagenesis[4, 5]. Copper has two stable isotopes, ^{63}Cu and ^{65}Cu, and its isotopic composition is reported as $\delta^{65}Cu(‰) = [(^{65}Cu/^{63}Cu)_{sample}/(^{65}Cu/^{63}Cu)_{NIST\ SRM\ 976}-1]\times10^3$. To date, only a few vertical profiles of dissolved $\delta^{65}Cu$ in the ocean have been reported[6, 7, 8, 9]. The reported $\delta^{65}Cu$ values (0.44−1.44‰) were substantially heavier than typical values for the solid Earth (~0‰)[10, 11]. However, as there were relatively large uncertainties in the reported data, it has been difficult to elucidate intra-ocean distributions. This is partly due to analytical difficulties in the determination of $\delta^{65}Cu$ caused by the interference of matrices and the inapplicability of the so-called double-spike technique.

Recently, we developed a simple and precise analytical method for $\delta^{65}Cu$ based

on a chelating resin extraction technique[12]. Here, we use this method to present new data of isotopic compositions of dissolved Cu (δ^{65}Cu) in seawater from the North/South Atlantic, South Indian, and North Pacific. We also present new data of rainwater samples collected from urban and rural regions. Using these data, the Cu isotopic composition in surface seawater is explained in an oceanographic context. In deep seawater, δ^{65}Cu values show a liner correlation with apparent oxygen utilisation (AOU), which suggests δ^{65}Cu becomes heavier along oceanic circulation because of preferential scavenging of the lighter isotope (i.e., ^{63}Cu). These are the first data showing that the stable isotopic composition of trace metals changes systematically with the age of deep water. Additionally, we propose a new box model for Cu in the ocean based on the combination of Cu concentration and δ^{65}Cu, which successfully constrains the marine biological cycling of Cu.

Results

Seawater analyses

The observed oceanic stations are shown in Fig. 1. All seawater data are summarised in Supplementary Table 1. The vertical profiles of dissolved Cu concentration and δ^{65}Cu for each station are presented in Supplementary Fig. 1, and

representative profiles are shown in Fig. 2. The Cu concentrations were in the range of 0.6−4.6 nmol kg^{-1}, and the profile at station ER10 agreed well with that determined in separate samples collected at the same station in our previous research (Supplementary Fig. 2)[14]. The δ^{65}Cu values ranged from +0.41‰ to +0.85‰, which were smaller than values determined by a $Mg(OH)_2$ co-precipitation technique (+0.50−1.44‰)[7, 8] at other stations and similar to values determined by a solvent extraction technique (+0.44−0.78‰)[6, 9] at other stations (Supplementary Fig. 3). The vertical samples from BATS have been analysed using a solvent extraction technique by Thompson et al.[9]. The reported δ^{65}Cu value (0.56±0.09‰) for a 2000 m depth sample was higher than our value (0.41±0.05‰). Unfortunately, we are not able to investigate the causes because the BATS samples have been exhausted. Recently, we performed intercalibration of δ^{65}Cu with a group from ETH, Zurich (see Acknowledgements section for details) using seawater collected at a station near the Japan Trench, of which the details are described in Supplementary Methods. The ETH group used a new method based on $Al(OH)_3$ co-precipitation[15], which gave results consistent to ours (Supplementary Fig. 4).

The vertical profiles of δ^{65}Cu in this work showed a common feature: δ^{65}Cu was ~0.5‰ in the surface layer and became heavier at depth. Station BD21 above the Juan de Fuca Ridge had a minimum Cu concentration at a depth of 2300 m, reflecting

the effect of a hydrothermal plume[16]. There were, however, no significant variations in δ^{65}Cu.

Rainwater analyses

We also determined δ^{65}Cu in rainwater for the first time (Table 1). Rainwater was sampled from rural and urban regions in Japan. The dissolved δ^{65}Cu values were in the narrow range of −0.12–+0.03‰ and did not show significant differences depending on location and time, whereas the Cu concentrations varied largely (1.1−23.5 nmol kg^{-1}), which may reflect various contributions of anthropogenic input. It has been reported that δ^{65}Cu values were ~0 ‰ for leachable fractions of marine aerosols[11] and bulk loess[17]. Rainwater would scavenge both atmospheric dusts and anthropogenic aerosols during precipitation. Therefore, it seems reasonable to presume the δ^{65}Cu value for atmospheric input to be zero.

Copper isotopes in surface seawater

In Fig. 3, the δ^{65}Cu in surface seawater is plotted against the reciprocal Cu concentration together with the ranges and averages of deep seawater, rural rainwater, and river water[8]. Assuming that average surface seawater is a mixture of average rural

rainwater, average river water, and average deep seawater, the plot would be located in the magenta triangle. Evaporation that is another important factor to control salinity; it would increase the Cu concentration but not change the δ^{65}Cu. However, the surface water data are shifted to the right of the triangles, indicating there must be other processes that decrease the dissolved Cu concentration (up to one tenths) while keeping the δ^{65}Cu values constant. The most likely process is phytoplankton uptake and adsorption of Cu onto the phytoplankton surface. It is well known that these processes produce biogenic sinking particles in the surface layer and they transport trace metals to the deep layer. Our data suggest that uptake and adsorption by phytoplankton in the open ocean does not cause significant fractionation of Cu isotopes. To clarify mechanisms controlling the Cu concentration and δ^{65}Cu, it is informative to compare Cu and Cd in the ocean. For vertical profiles of dissolved Cd, the isotopic ratio (ε^{114}Cd) correspondingly increases with a decrease in the concentration in the surface layer and decreases with an increase in the concentration from the surface to the intermediate layer, because biological uptake causes isotopic fractionation of Cd[18, 19, 20]. Therefore, the profile of ε^{114}Cd from the surface to the intermediate layer becomes a mirror image of the concentration, and ε^{114}Cd linearly correlates with the logarithm concentration in the surface layer because of Rayleigh fractionation during biological uptake[18, 19, 20, 21].

However, δ^{65}Cu does not change uniformly with respect to the Cu concentration from the surface to the intermediate layer (Fig. 2 and Supplementary Fig. 1), and does not correlate with the logarithmic concentration in the surface layer (Supplementary Fig. 5). These facts also indicate biological processes cause insignificant fractionation of the Cu isotopes.

Copper isotopes in deep seawater

Given that uptake and adsorption of Cu by phytoplankton does not cause fractionation of Cu isotopes, biogenic sinking particles would have the same δ^{65}Cu value as surface seawater. Copper regenerated through decomposition of the biogenic sinking particles should produce δ^{65}Cu values in deep seawater, which are the same as those in surface seawater under this assumption. However, observed δ^{65}Cu in deep seawater is heavier than that in surface seawater. In addition, the profiles of δ^{65}Cu are similar to those of apparent oxygen utilisation (AOU; Fig. 2 and Supplementary Fig. 1). All δ^{65}Cu values are plotted against AOU, revealing a positive correlation (R^2 = 0.60, n = 77; Fig. 4a). In the layer deeper than 2000 m, δ^{65}Cu vs. AOU shows a stronger correlation (R^2 = 0.70, n = 25; Fig. 4b). Because AOU is a measure of the age of deep water, these data imply that δ^{65}Cu increases through deep water circulation. When the

Cu concentration is plotted against AOU, there is also a weak correlation (R^2 = 0.31, n = 77, Fig. 5).

In the case of Cd, the dissolved concentration is very low (~0.001 nmol kg^{-1}) in the surface layer because of biological uptake, and it is high in the deep layer (~1 nmol kg^{-1}) because of remineralisation from biogenic particles; it also increases along the global deep circulation[3]. Because there is a significant correlation between Cd and phosphate, the distribution of Cd is dominated by biogeochemical recycling. The isotopic composition of Cd is heavier in surface seawater ($\varepsilon^{114/110}$Cd = 10–40 with respect to a JMC Cd Münster solution) than in deep seawater ($\varepsilon^{114/110}$Cd = ~3) that is almost uniform in the world ocean[18, 19, 20]. Biological uptake depletes the Cd concentration and preferentially leaves isotopically heavy Cd in surface seawater. It is suggested that Cd in a replenished surface seawater reservoir is originally characterised by $\varepsilon^{114/110}$Cd = ~3 and that this Cd is almost quantitatively transported by biogenic sinking particles from the surface to depth and remineralised in deep water; thus, the Cd isotopic composition of deep water is homogeneous, whereas the Cd concentration increases along with deep water circulation.

The δ^{65}Cu in deep seawater appears to be controlled by a ubiquitous effect throughout the water column and deep water pathway because δ^{65}Cu correlates with

AOU. Copper is more strongly scavenged than other recycled-type trace metals such as Cd[3, 5]. The scavenging is likely the reason that δ^{65}Cu is heavy in the deep layer and becomes heavier with the age of deep seawater. If this is true, ^{63}Cu would be preferentially adsorbed to sinking particles and preserved in sinks. The low linearity of Cu concentration against AOU (Fig. 5) would be due to the combination of scavenging throughout the water column and supply from sediments through decomposition of the organic fraction of sinking particles. The Cu released from sediments most likely has a δ^{65}Cu value similar to that in seawater near the bottom, resulting in the linearity of δ^{65}Cu vs. AOU.

Box model for Cu in the modern ocean

We present a new box model for Cu based on both concentration and isotopic composition (Fig. 6 and Supplementary Table 2). This model assumes a steady-state for the modern ocean. In this model, the global ocean is divided simply into a euphotic layer and a deep layer at a depth of 100 m. A thin layer on the sediment surface is considered as the box of the 'scavenged layer', where organic matter is decomposed during early diagenesis[22]. In Fig. 6, the black figures are observed or previously published values, as described below. Magenta figures are values calculated using the

following equations[11], which assumes a steady-state for each box:

$$\Sigma F_{in} = \Sigma F_{out}$$

$$\Sigma F_{in}\delta_{in} = \Sigma F_{out}\delta_{out}$$

where F_{in} and F_{out} represent an input and output flux for the box, and δ_{in} and δ_{out} represent δ^{65}Cu values of F_{in} and F_{out}, respectively. Based on this work, the depth-weighted averages of Cu concentration and δ^{65}Cu are 1.1 nmol kg^{-1} and 0.49‰ in surface seawater and 2.5 nmol kg^{-1} and 0.60‰ in deep seawater, respectively. The water mixing rate between the upper box and lower box is assumed to be 1.2×10^{15} m^3 year^{-1}, which has been determined from ^{14}C data[23]. We assumed that the main inputs of dissolved Cu to the ocean are riverine and atmospheric inputs. The reported riverine input of dissolved Cu to the ocean among four studies[4, 8, 24, 25] was in the range of $6–9\times10^8$ mol year^{-1}, and the average value of 7.6×10^8 mol year^{-1} was applied to our model. The removal rate of dissolved Cu from the ocean was estimated to be ~4.0 nmol kg^{-1} year^{-1} by using a vertical advection diffusion model[4, 5]. By multiplying this value by the total ocean volume (1.35×10^{21} kg), the scavenging flux of Cu in the ocean was estimated to be 5.4×10^9 mol year^{-1}. Riverine input δ^{65}Cu was determined in rivers worldwide; the rivers account for approximately one-quarter of all riverine discharge to the ocean[8]. The discharge-weighted average of 0.68‰ of these rivers was used in our

193 model. The δ^{65}Cu of atmospheric input was assumed to be 0‰ because δ^{65}Cu values are
194 ~0‰ for rainwater, leachable fractions of marine aerosols[11], and loess[17]. It was assumed
195 that the δ^{65}Cu of sinking particles (of mainly biogenic origin) from surface water was
196 the same as the δ^{65}Cu of ambient surface seawater (i.e., 0.49‰), because isotopic
197 fractionation during phytoplankton uptake and adsorption onto phytoplankton surface is
198 expected to be insignificant, as described above. The δ^{65}Cu of the benthic flux from the
199 scavenged layer to deep seawater was assumed to be the global average of 0.58‰. This
200 value is the average of δ^{65}Cu in seawater samples nearest the bottom of the ocean. The
201 unknown Cu fluxes that were calculated by this model are those of supply from the
202 atmosphere, transport by sinking particles from the surface, preservation in sediments,
203 and return from the scavenged layer to deep water. The unknown δ^{65}Cu values
204 calculated by this model are those of the transporting flux by sinking particles in deep
205 water and the preserved flux into sediments.
206

207 ## Discussion

208 From our data we infer that the δ^{65}Cu values in surface seawater are mainly
209 controlled by supply from rivers, atmosphere, and deep seawater. Biological uptake
210 does not cause significant isotopic fractionation of Cu in the open ocean. δ^{65}Cu values

211 in deep seawater are heavier than those in surface seawater and become heavier with the
212 age of deep seawater because of preferential scavenging for the light isotope (^{63}Cu).

213 Biological fractionation of Cu isotopes has not yet been sufficiently clarified in
214 the literature. There are only a few studies concerning isotopic fractionation of Cu by
215 phytoplankton. Laboratory experiments have shown that uptake by several diatoms
216 caused no significant fractionation or slight enrichment of the heavy Cu isotope (^{65}Cu)
217 when the initial Cu concentration was ~200 nmol L^{-1} (ref. 26). However, a geochemical
218 study in the Garonne River suggested that diatom species prefer the light Cu isotope
219 (^{63}Cu)[27]. Thus, it is necessary to determine the δ^{65}Cu of natural phytoplankton in the
220 open ocean in future work.

221 We suggest that Fe-Mn oxides may be a major sink of Cu in the oxic ocean.
222 δ^{65}Cu values of Fe-Mn nodules are 0.33±0.23‰ (ave±2-sd, n = 14) in the Pacific,
223 0.25±0.26‰ (n = 8) in the Atlantic, and 0.31±0.23‰ (n = 31) in the world ocean[10]; the
224 δ^{65}Cu values of Fe-Mn crusts are 0.54±0.07‰ (n = 8) in the Pacific, 0.33±0.15‰ (n =
225 8) in the Atlantic, and 0.44±0.23‰ (n = 16) in the world ocean[11]. Thus, δ^{65}Cu of Fe-Mn
226 crusts and nodules is lighter than that of dissolved Cu in the ocean. Furthermore, the
227 δ^{65}Cu of Fe-Mn crusts is significantly heavier in the Pacific than in the Atlantic (p =
228 0.01). These data are consistent with preferential scavenging of ^{63}Cu and gradual

229 accumulation of ^{65}Cu in seawater through the global ocean circulation. This view,
230 however, seems contrary to experimental results on adsorption of Cu isotopes on Fe
231 oxyhydroxides[26, 28], which indicate enrichment of the heavy Cu isotope onto oxide
232 surfaces in $NaNO_3$ solutions or mixtures of acidic drainage and river water. The
233 discrepancy may be caused by differences in conditions, such as pH, Cu concentration,
234 and organic ligands concentration, between experimental solutions and natural seawater.
235 Additionally, it was found that Cu is associated with Mn and not Fe in Fe-Mn crusts[29].
236 Isotopic fractionation between free Cu and organic ligand-bound Cu would also be
237 important for Cu isotopes in seawater, because Cu is mostly complexed with organic
238 ligands. In a laboratory experiment, humic acid preferentially complexes with the heavy
239 Cu isotope[30]. Therefore, it is likely that the complexation of Cu with dissolved organic
240 ligands in seawater also causes mass fractionation of Cu, because the organic ligands
241 and humic acid most likely have the same functional groups. Furthermore, Cu is
242 contained not only in the Fe-Mn oxide fraction but also in the organic fraction of
243 sinking particles[31, 32]. Thus, understanding isotopic fractionation during scavenging of
244 dissolved Cu from seawater is not straightforward. It was originally proposed in a
245 previous field study of rivers and oceans that there is equilibrium partitioning of
246 isotopes between heavy Cu bound to organic ligands in the dissolved phase and light Cu

247 adsorbed to particles[8]. This hypothesis is consistent with our explanation of light Cu
248 scavenging.

249 In the box model using both the Cu concentration and δ^{65}Cu (Fig. 6), we
250 constrained the transporting flux of Cu from surface to deep water by sinking particles
251 to be 3.4×10^{9} mol year^{-1}. The residence time for dissolved Cu in surface water (<100 m)
252 is ~9 years, which is consistent with previous estimates of 3.2−11.7 years[5, 33]. The
253 calculated preservation flux of Cu into sediments is 1.7×10^{8} mol year^{-1}. The overall
254 residence time of Cu in the ocean is calculated by dividing the average concentration by
255 the preservation flux. Our estimate of the overall residence time of Cu is 2000 years,
256 which is within the range of literature values (1700−6400 years)[4, 11]. The calculated
257 δ^{65}Cu of preserved Cu in sediments is +0.30‰, which is quite similar to the averages
258 reported for Fe-Mn oxides[10, 11].

259 We also constrained the atmospheric input of dissolved Cu to be 9.6×10^{8} mol
260 year^{-1}. Our model suggests that the present atmospheric input of Cu is comparable to
261 the riverine input. A significant correlation was found between Cu and ^{210}Pb in surface
262 seawater, implying a strong atmospheric supply of Cu because ^{210}Pb is a tracer for
263 atmospheric input[4]. These authors estimated both the atmospheric and riverine Cu input
264 to be 6.0×10^{8} mol year^{-1}, which is similar to our results. However, our value is

265 significantly larger than the natural atmospheric input previously estimated at 5.4×10^7
266 mol $year^{-1}$, which was obtained by multiplying the total dust flux by the mean crustal
267 Cu concentration and solubility[11].

268 Two possible explanations are given to rationalise this difference. First, it is
269 possible that the Cu concentration and solubility in marine aerosols would be different
270 from those in the continental crust. The enrichment factor of Cu relative to Al in marine
271 aerosols varies over a large range of 1−200 compared with the continental crust[25]. The
272 solubility of Cu in aerosols has a wide range of 15−86%[34]. It was suggested that the
273 enriched and soluble Cu in aerosols is from anthropogenic sources[34, 35, 36]. However,
274 Maring et al. evaluated the source of Cu enrichment in aerosols near Enewetak in the
275 North Pacific, suggesting that atmospheric soluble Cu is from primary natural origins
276 and that soil organic matter enriched in Cu could be a significant source of soluble Cu[37].
277 If anthropogenic Cu has significantly affected atmospheric input as we estimated, then
278 the steady-state assumption is imperfect for the modern ocean, because anthropogenic
279 inputs would have substantially increased in the recent ~100 years, whereas the overall
280 oceanic residence time of Cu is approximately 1000 years. Second, other fluxes to open
281 ocean surface may be suggested. One possible flux is from the continental shelf
282 sediment, where a portion of Cu is derived from the reduction of primary terrigenous

283 metal oxides[38]. The δ^{65}Cu value of this flux would also be close to the crustal value
284 (0‰) and lighter than that of surface seawater. If these fluxes are included in our box
285 model, then our estimate of atmospheric input may decrease. As described above, some
286 uncertainties remain in our box model. Our results, however, confirm possibilities of
287 this new box model based on both concentration and isotopic composition of trace
288 metals.
289
290 ## Methods
291 ### Seawater samples
292 The South Indian and North Pacific seawater samples were collected during the
293 R/V *Hakuho-maru* voyages KH 09-4, KH 10-2, KH 11-7, and KH 12-4 using a clean
294 sampling system[14]. In a clean booth, seawater was filtered through a 0.2 μm cartridge
295 (Acro pak, Poll), acidified with HCl to pH 1.7−2.2, and stored in 2 L or 4 L LDPE
296 bottles (Nalge Nunc) or 6 L LDPE cubic bags (Lontainer, Sekisui Seikei), which were
297 pre-cleaned by overnight treatment with 4 M HCl followed by rinsing with deionised
298 water. The North Atlantic sample was a GEOTRACES reference material collected at
299 BATS during the US-GEOTRACES KN193-5 voyage of the R/V *Knorr*. The South
300 Atlantic sample was collected at Station 3 during the UK-GEOTRACES D357 voyage

301 of the RSS *Discovery*.

302

303 **Rainwater samples**

304 Rainwater was collected from two sites using pre-cleaned polyethylene funnels
305 and cubic bags (Lontainer) or 2 L LDPE bottles. One site was on the roof of the main
306 building of the Institute for Chemical Research, which is located in an urban area of the
307 Main Island, Japan. The other site was on top of Mt. Kajigamori, which is located in a
308 rural area of Sikoku Island. Rainwater samples were filtered through a 0.22 μm filter
309 (Millipore) and acidified with HCl to pH 1.7−2.1.

310

311 **Analytical procedure of δ^{65}Cu and Cu**

312 Copper concentration and isotopic composition were determined as described
313 in a previous paper[12]. Briefly, Cu in seawater or rainwater was collected using a column
314 of Nobias chelate PA-1 resin (Hitachi High Technologies) followed by elution with 1 M
315 HNO_3. The eluate was evaporated to dryness, and the residue was re-dissolved with 10
316 M HCl. The sample was passed through a column of anion exchange resin (AG MP-1,
317 Bio-Rad); additional 10 M HCl was then passed through the column to remove
318 co-existing elements, followed by the elution of Cu with 5 M HCl. This eluate was

evaporated to dryness and the residue was re-dissolved with 1 M HNO_3. Finally, the 1 M HNO_3 solution was re-evaporated and the residue was re-dissolved with 0.4 M HNO_3, yielding the pre-concentrated sample. One hundred micrograms of the pre-concentrated sample was diluted with 0.4 M HNO_3 by a factor of ~10 and used for measurement of Cu concentration. Co-existing Na, Mg, Ba, Ni, Zn, Cr, and Ti were also measured to ascertain whether these interfering elements possessed concentrations sufficiently low to permit accurate Cu isotopic measurements. When the Na (ppb)/Cu (ppb) ratio in the pre-concentrated sample was higher than 1, the solution was not used for discussion. For the Cu isotopic measurement, which used a multicollector ICP-MS (Thermo Finnigan Neptune or Neptune Plus), the final solution was diluted to adjust the Cu concentration to 50 ppb and Zn was added to give a solution of 100 ppb for external normalisation. The precision of this method was evaluated previously by repeated analyses of coastal seawater to be ±0.07‰ (±2-sd, n = 6)[12]. In this study, 34 samples were each divided into two aliquots and analysed in duplicate, resulting in an average 2-sd of 0.045 ‰ (n = 34) for δ^{65}Cu and 0.11 nmol kg^{-1} (n = 34) for Cu concentration. These values are shown as error bars in the figures.

References

1. Brand LE, Sunda WG & Guillard RRL. Reduction of marine phytoplankton reproduction rates by copper and cadmium. *J. Exp. Biol. Ecol.* **96**, 225-250 (1986).

2. Coale KH & Bruland KW. Copper complexation in the Northeast Pacific. *Limnol. Oceanogr.* **33**, 1084-1101 (1988).

3. Bruland KW & Lohan MC. Controls of Trace Metals in Seawater. In: *Treatise on Geochemistry* (ed^(eds Holland HD, Turekian KK). Elsevier (2003).

4. Boyle EA, Sclater FR & Edmond JM. The distribution of dissolved copper in the Pacific. *Earth Planet. Sci. Lett.* **37**, 38-54 (1977).

5. Bruland KW. Oceanographic distributions of cadmium, zinc, nickel, and copper in the North Pacific. *Earth Planet. Sci. Lett.* **47**, 176-198 (1980).

6. Boyle EA, *et al.* GEOTRACES IC1 (BATS) contamination-prone trace element isotopes Cd, Fe, Pb, Zn, Cu, and Mo intercalibration. *Limnol. Oceanogr,*

Methods **10**, 653-665 (2012).

7. Bermin J, Vance D, Archer C & Statham PJ. The determination of the isotopic composition of Cu and Zn in seawater. *Chem. Geol.* **226**, 280-297 (2006).

8. Vance D, *et al.* The copper isotope geochemistry of rivers and the oceans. *Earth Planet. Sci. Lett.* **274**, 204-213 (2008).

9. Thompson CM, Ellwood MJ & Wille M. A solvent extraction technique for the isotopic measurement of dissolved copper in seawater. *Anal. Chim. Acta* **775**, 106-113 (2013).

10. Albarède F. The Stable Isotope Geochemistry of Copper and Zinc. In: *Geochemistry of Non-Traditional Stable Isotopes* (ed^(eds Johnson CM, Beard BL, Albarède F). Mineralogical Society of America (2004).

11. Little SH, Vance D, Walker-Brown C & Landing WM. The oceanic mass balance of copper and zinc isotopes, investigated by analysis of their inputs, and

outputs to ferromanganese oxide sediments. *Geochim. Cosmochim. Acta* **125**, 673-693 (2014).

12. Takano S, Tanimizu M, Hirata T & Sohrin Y. Determination of isotopic composition of dissolved copper in seawater by multi-collector inductively coupled plasma mass spectrometry after pre-concentration using an ethylenediaminetriacetic acid chelating resin. *Anal. Chim. Acta* **784**, 33-41 (2013).

13. Schlitzer R. Ocean Data View. http://www.awi-bremerhaven.de/GEO/ODV (2002).

14. Vu HTD & Sohrin Y. Diverse stoichiometry of dissolved trace metals in the Indian Ocean. *Sci. Rep.* **3**, 1745 (2013).

15. Zhao Y, Vance D, Abouchami W & de Baar HJW. Biogeochemical cycling of zinc and its isotopes in the Southern Ocean. *Geochim. Cosmochim. Acta* **125**, 653-672 (2014).

16. Lupton J. Hydrothermal helium plumes in the Pacific Ocean. *J. Geophys. Res.* **103**, 15853-15868 (1998).

17. Li W, Jackson SE, Pearson NJ, Alard O & Chappell BW. The Cu isotopic signature of granites from the Lachlan Fold Belt, SE Australia. *Chem. Geol.* **258**, 38-49 (2009).

18. Abouchami W, *et al.* Biogeochemical cycling of cadmium isotopes in the Southern Ocean along the Zero Meridian. *Geochim. Cosmochim. Acta* **127**, 348-367 (2014).

19. Ripperger S, Rehkämper M, Porcelli D & Halliday AN. Cadmium isotope fractionation in seawater — A signature of biological activity. *Earth Planet. Sci. Lett.* **261**, 670-684 (2007).

20. Xue Z, *et al.* Cadmium isotope variations in the Southern Ocean. *Earth Planet. Sci. Lett.* **382**, 161-172 (2013).

21. Abouchami W, *et al.* Modulation of the Southern Ocean cadmium isotope signature by ocean circulation and primary productivity. *Earth Planet. Sci. Lett.* **305**, 83-91 (2011).

22. Chester R, Thomas A, Lin FJ, Basaham AS & Jacinto G. The solid state speciation of copper in surface water particulates and oceanic sediments. *Mar. Chem.* **24**, 261-292 (1988).

23. Sarmiento JL. *Ocean Biogeochemical Dynamics*. Princeton University Press (2006).

24. Gaillardet J, Viers J & Dupré B. 5.09 - Trace Elements in River Waters. In: *Treatise on Geochemistry* (ed^(eds Holland HD, Turekian KK). Elsevier (2003).

25. Chester R & Jickells T. *Marine Geochemistry*. Willey-Blackwell (2012).

26. Pokrovsky OS, Viers J, Emnova EE, Kompantseva EI & Freydier R. Copper

isotope fractionation during its interaction with soil and aquatic microorganisms and metal oxy(hydr)oxides: Possible structural control. *Geochim. Cosmochim. Acta* **72**, 1742-1757 (2008).

27. Petit JCJ, *et al.* Anthropogenic sources and biogeochemical reactivity of particulate and dissolved Cu isotopes in the turbidity gradient of the Garonne River (France). *Chem. Geol.* **359**, 125-135 (2013).

28. Balistrieri LS, Borrok DM, Wanty RB & Ridley WI. Fractionation of Cu and Zn isotopes during adsorption onto amorphous Fe(III) oxyhydroxide: Experimental mixing of acid rock drainage and ambient river water. *Geochim. Cosmochim. Acta* **72**, 311-328 (2008).

29. Little SH, Sherman DM, Vance D & Hein JR. Molecular controls on Cu and Zn isotopic fractionation in Fe–Mn crusts. *Earth Planet. Sci. Lett.* **396**, 213-222 (2014).

30. Bigalke M, Weyer S & Wilcke W. Copper isotope fractionation during

complexation with insolubilized humic acid. *Environ. Sci. Technol.* **44**, 5496-5502 (2010).

31. Fischer K, Dymond J, Lyle M, Soutar A & Rau S. The benthic cycle of copper: Evidence from sediment trap experiments in the eastern tropical North Pacific Ocean. *Geochim. Cosmochim. Acta* **50**, 1535-1543 (1986).

32. Noriki S, Shiribiki T, Yokomizo H, Harada K & Tsunogai S. Copper and nickel in settling particle collected with sediment trap in the western North Pacific. *Geochem. J.* **31**, 373-382 (1997).

33. Helmers E & Schrems O. Wet deposition of metals to the tropical North and the South Atlantic ocean. *Atmos. Environ.* **29**, 2475-2484 (1995).

34. Duce RA, *et al.* The atmospheric input of trace species to the world ocean. *Global Biogeochem. Cycles* **5**, 193-259 (1991).

35. Arimoto R, Ray BJ, Duce RA, Hewitt AD, Boldi R & Hudson A. Concentrations,

sources, and fluxes of trace elements in the remote marine atmosphere of New Zealand. *Journal of Geophysical Research: Atmospheres* **95**, 22389-22405 (1990).

36. Desboeufs KV, Sofikitis A, Losno R, Colin JL & Ausset P. Dissolution and solubility of trace metals from natural and anthropogenic aerosol particulate matter. *Chemosphere* **58**, 195-203 (2005).

37. Maring HB & Duce RA. The impact of atmospheric aerosols on trace metal chemistry in open ocean surface seawater: 2. Copper. *J. Geophys. Res.* **94**, 1039-1045 (1989).

38. Boyle EA, Huested SS & Jones SP. On the distribution of copper, nickel, and cadmium in the surface waters of the North Atlantic and North Pacific Ocean. *J. Geophys. Res.* **86**, 8048-8066 (1981).

Acknowledgements

We would like to thank Susan Little, Corey Archer, and Derek Vance (ETH, Zurich) for performing intercalibration with us and providing the South Atlantic sample. We also thank the officers and crew of the R/V *Hakuho-Maru* for their assistance in obtaining samples and Shoji Imai (The University of Tokushima) for sampling rainwater at the top of Mt. Kajigamori. We are grateful to Takanori Nakano and Kichoel Shin (Research Institute for Humanity and Nature) for their help with the MC-ICP-MS measurements. This work was supported by funds from the Steel Industry Foundation for the Advancement of Environmental Protection Technology and by grants-in-aids from the Japanese Society for the Promotion of Science.

Author contributions

S.T. and Y.S. designed the research. S.T. determined the concentration of Cu and δ^{65}Cu. M.T. contributed to measurements with MC-ICP-MS. T.H helped with the development of the analytical method and supplied the standard reference material of Cu (NIST SRM 976). All authors contributed to the interpretation of the data and preparation of the manuscript.

Competing financial interests

The authors declare no competing financial interests.

Figure legends

Figure 1 Station locations. Samples for the analysis of $\delta^{65}Cu$ were collected at these stations during R/V *Hakuho-maru* voyages. The numbers of samples are 10 at TR7, 10 at TR15, 10 at CR27, 14 at BD17, 12 at BD21, and 18 at ER10. This figure was produced with Ocean Data View[13].

Figure 2 Representative vertical profiles of the concentration and isotopic composition of Cu. Magenta triangles indicate Cu concentration. Blue squares and black circles indicate $\delta^{65}Cu$ and apparent oxygen utilisation (AOU), respectively. Black diamonds indicate fluorescence or chlorophyll a (Chl. a). The error bars are 2-sd of ±0.045‰ for $\delta^{65}Cu$ and ±0.11 nmol kg^{-1} for Cu concentration, as described in the Methods section. The vertical profiles at all stations are shown in Supplementary Fig. 1.

Figure 3 $\delta^{65}Cu$ versus reciprocal Cu concentration for surface seawater (<100 m). The error bars of the magenta circles are 2-sd of ±0.045‰. The blue, black, and orange

518 shaded areas indicate the ranges of the data for deep seawater, river water, and rural rain,
519 respectively. The magenta triangle indicates the possible range of mixtures of average
520 deep seawater, river water, and rainwater. The surface water data shifted to the right of
521 the triangle indicate that other processes decrease the dissolved Cu concentration in the
522 surface seawater.
523
524 Figure 4 δ^{65}Cu versus AOU for seawater. The error bars for δ^{65}Cu are 2-sd of ±0.045‰.
525 (a) All δ^{65}Cu values were plotted against AOU. The solid line was determined by a
526 regression analysis of all plots: $\delta^{65}Cu = 0.00067 \times AOU + 0.50$, $R^2 = 0.60$, $n = 77$, $p <$
527 0.001. (b) δ^{65}Cu values were plotted against AOU in deep seawater (>2000 m). The
528 solid line was determined by a regression analysis of all plots: $\delta^{65}Cu = 0.0016 \times AOU +$
529 0.32, $R^2 = 0.70$, $n = 25$, $p < 0.001$.
530
531 Figure 5 Cu concentration versus AOU in the ocean. The error bars are 2-sd of ±0.11
532 nmol kg^{-1}. The solid line was defined as: $[Cu] = 0.0046 \times AOU + 1.5$, $R^2 = 0.31$, $n = 77$,
533 $p < 0.001$.
534

Figure 6 Box model for Cu cycling in the ocean based on both elemental concentration and isotopic ratio. The Roman and italic values below the process names represent Cu flux in units of 10^9 mol $year^{-1}$ and $\delta^{65}Cu$ values, respectively. Black figures indicate observed values and magenta figures indicate values calculated based on mass balance.

Table

Table 1 Rainwater analysis results

Sample [a]	Date	Cu [nmol kg^{-1}]	$\delta^{65}Cu$
Urban-1	3 Jul 2013	23.46	−0.12
Urban-2	20 Jun 2013	1.51	−0.08
Urban-3	26 Jun 2013	1.84	0.03
Rural-1	16 Jun 2013	1.12	−0.03
Rural-1	16 Jun 2013	1.14	−0.01
Rural-2	8 Jul 2013	2.60	0.03

[a] 'Urban' samples were collected on the roof of the main building on the Uji campus on Main Island, Japan. 'Rural' samples were collected at the top of Mt. Kajigamori on Sikoku Island, Japan.

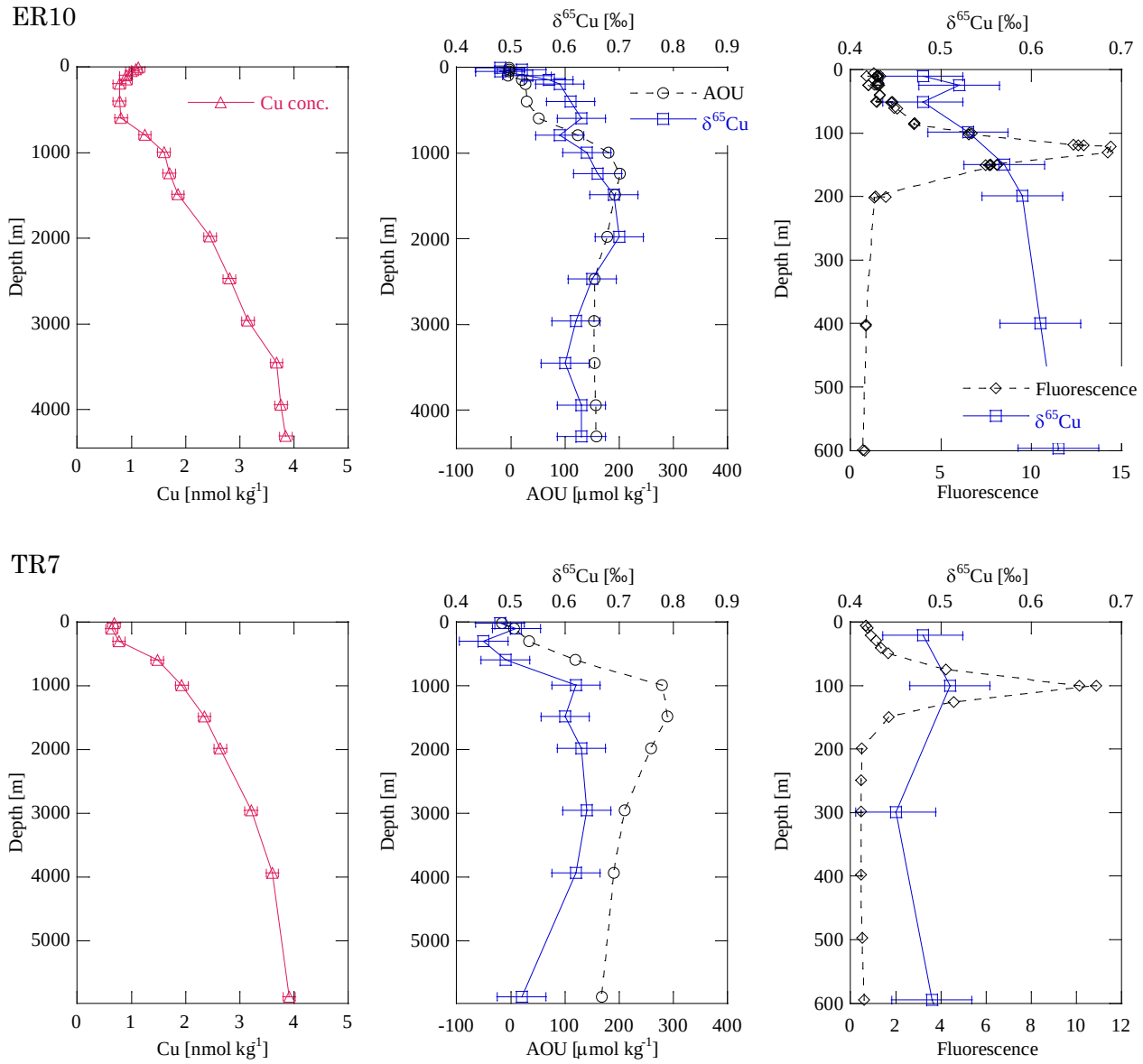

Supplementary Figure 1 Vertical profiles of Cu concentration, δ^{65}Cu, apparent oxygen utilisation (AOU), and fluorescence or chlorophyll a (Chl. a) in the ocean. Magenta triangles indicate Cu concentration. Blue squares and black circles indicate δ^{65}Cu and AOU, respectively. Black diamonds indicate Chl. a or fluorescence.

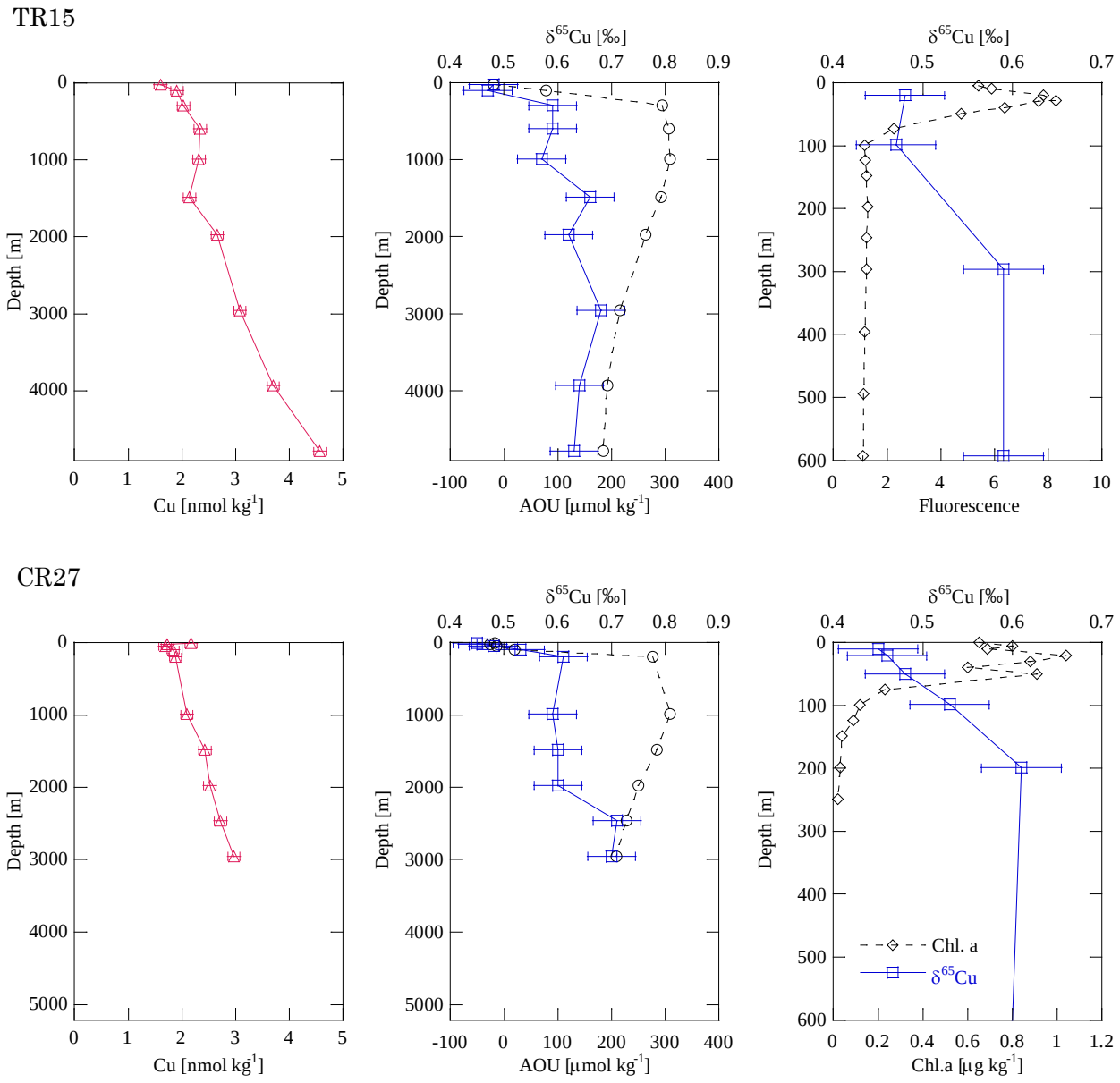

Supplementary Figure 1 (continued)

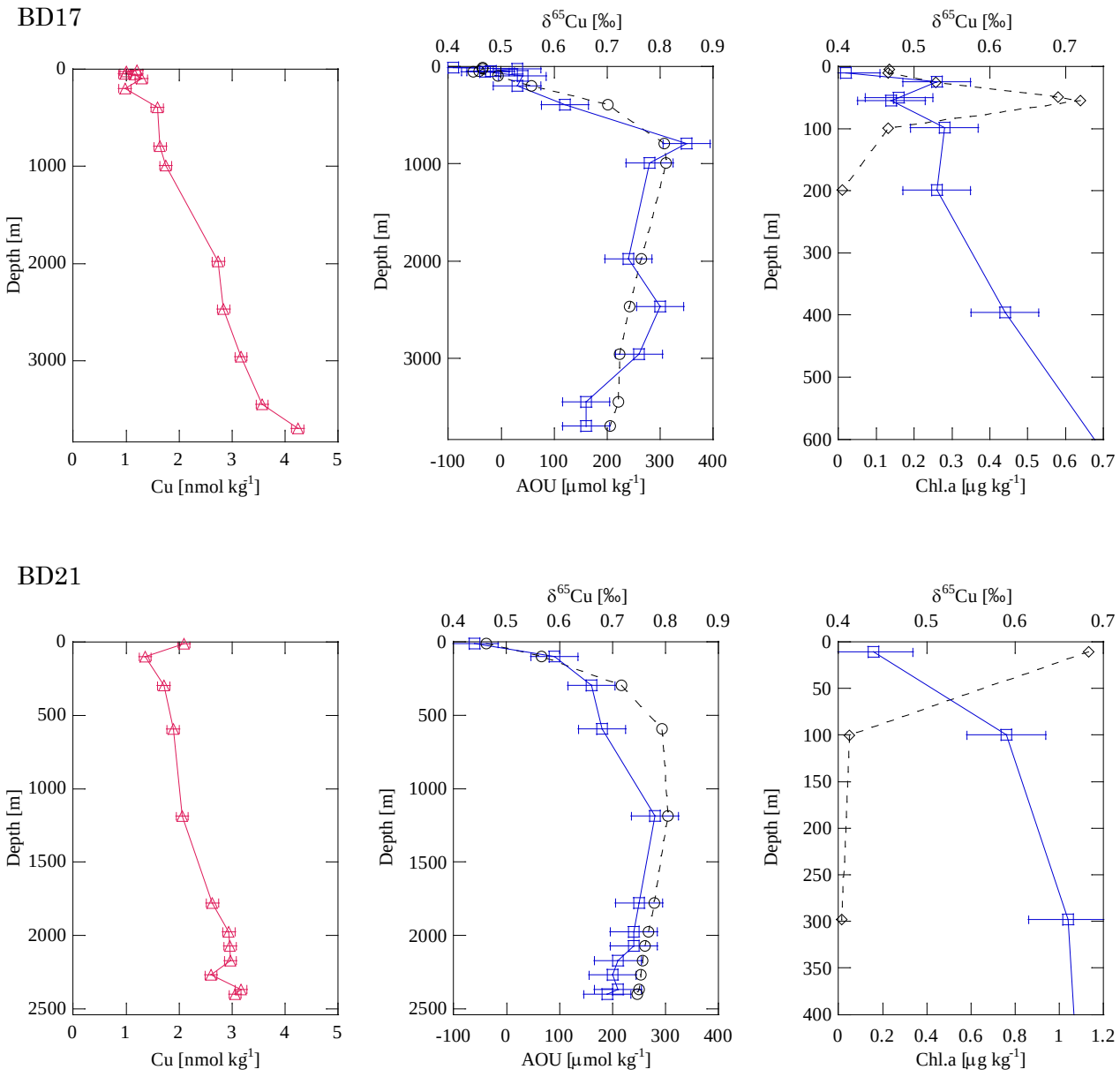

Supplementary Figure 1 (continued)

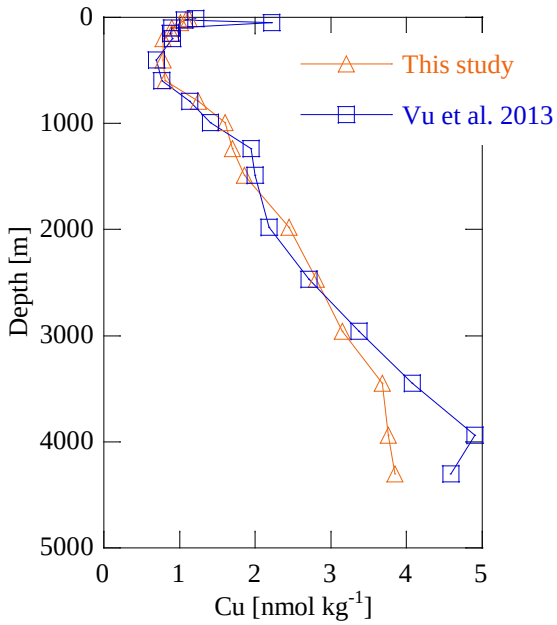

Supplementary Figure 2 Comparison of Cu concentration profiles at ER10 from a previous paper[1] and from this work. Blue squares and orange triangles represent data in the previous and present study, respectively.

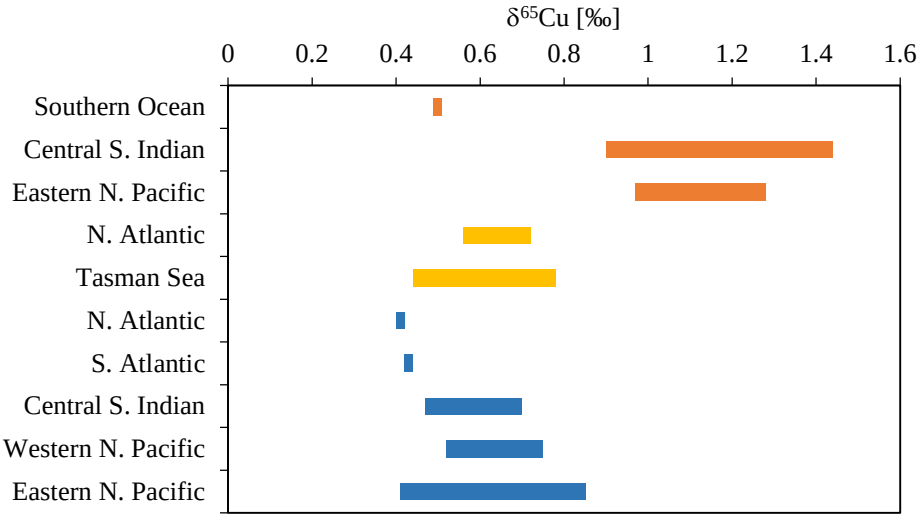

Supplementary Figure 3 Comparison of dissolved δ^{65}Cu ranges in seawater. Orange and yellow bars indicate the ranges reported by British (ETH at present)[2, 3] and Australian groups[4, 5], respectively. Blue bars indicate those in this study.

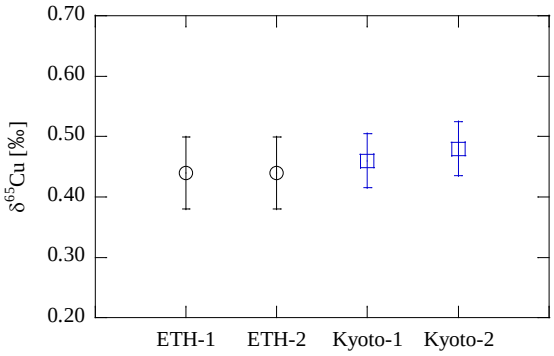

Supplementary Figure 4 Intercalibration of δ^{65}Cu in seawater between the method of the ETH group (black circles) and our method (blue squares). Uncertainties for the ETH methodology are based on repeated (n = 29) analyses of a secondary Cu standard over a period of 6 months. The seawater sample collected at a 7145 m depth near the Japan Trench was divided into 4 aliquots and analysed in duplicate with each method. The results were found to be consistent within uncertainties.

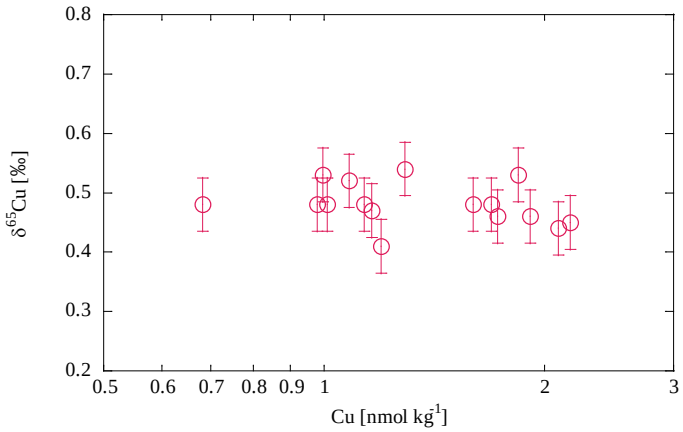

Supplementary Figure 5 The correlation between δ^{65}Cu and Cu concentration in the surface seawater (<100 m). Note that the horizontal axis is a logarithmic scale.

Supplementary Table 1 Seawater analysis results.

Depth [m]	First analysis		Second analysis		Average		2 s.d.	
	δ^{65}Cu [‰]	Cu [nmol kg^{-1}]	δ^{65}Cu [‰]	Cu [nmol kg^{-1}]	δ^{65}Cu [‰]	Cu [nmol kg^{-1}]	δ^{65}Cu [‰]	Cu [nmol kg^{-1}]
KH 11-7, TR7, 29.99N, 165.01E, depth 5883 m, 19 June 2011								
21	0.48	0.68			0.48	0.68		
100	0.49	0.63	0.53	0.66	0.51	0.64	0.05	0.04
299	0.48	0.77	0.43	0.77	0.45	0.77	0.07	0.00
595	0.48	1.47	0.51	1.50	0.49	1.48	0.03	0.05
991	0.67	1.94	0.58	1.92	0.62	1.93	0.12	0.02
1484	0.60	2.35			0.60	2.35		
1979	0.63	2.68	0.62	2.59	0.63	2.64	0.02	0.12
2958	0.67	3.19	0.61	3.22	0.64	3.21	0.09	0.05
3938	0.62	3.66	0.61	3.54	0.62	3.60	0.01	0.18
5882	0.54	3.95	0.50	3.87	0.52	3.91	0.06	0.11
KH11-7, TR15, 165.01°E, 51.00°N, depth 4802 m,27 June 2011								
20	0.46	1.59	0.50	1.61	0.48	1.60	0.06	0.03
99	0.46	1.90	0.46	1.93	0.46	1.91	0.00	0.04
296	0.61	2.03			0.61	2.03		
593	0.62	2.24	0.60	2.43	0.61	2.34	0.03	0.27
989	0.62	2.27	0.54	2.37	0.58	2.32	0.11	0.15
1482	0.70	2.25	0.62	2.02	0.66	2.14	0.12	0.32
1974	0.62	2.67			0.62	2.67		
2953	0.70	3.06	0.69	3.11	0.70	3.08	0.02	0.07
3929	0.65	3.51	0.67	3.90	0.66	3.70	0.04	0.54
4781	0.62	4.31	0.64	4.83	0.63	4.57	0.03	0.74
KH11-7, TR17, 143.87°E, 37.81°N, depth 7150 m, 30 June 2011								
7145	0.49	4.22	0.46	4.20	0.48	4.21	0.04	0.03

Supplementary Table 1 (continued)

Depth [m]	First analysis		Second analysis		Average		2 s.d.	
	$\delta^{65}Cu$ [‰]	Cu [nmol kg^{-1}]	$\delta^{65}Cu$ [‰]	Cu [nmol kg^{-1}]	$\delta^{65}Cu$ [‰]	Cu [nmol kg^{-1}]	$\delta^{65}Cu$ [‰]	Cu [nmol kg^{-1}]
KH-10-2, CR27, 159.99°E, 46.97°N, depth 5114 m, 29 June 2010								
10	0.46	2.21	0.45	2.13	0.45	2.17	0.00	0.11
21	0.45	1.78	0.47	1.68	0.46	1.73	0.03	0.15
50	0.46	1.71	0.50	1.68	0.48	1.69	0.05	0.04
99	0.52	1.92	0.54	1.77	0.53	1.84	0.04	0.21
199	0.63	1.90	0.59	1.87	0.61	1.88	0.05	0.05
990	0.60	2.10	0.58	2.09	0.59	2.09	0.03	0.02
1483	0.62	2.41	0.58	2.46	0.60	2.43	0.06	0.07
1974	0.60	2.57	0.60	2.48	0.60	2.52	0.01	0.12
2464	0.70	2.72	0.71	2.72	0.71	2.72	0.01	0.01
2954	0.72	2.99	0.68	2.95	0.70	2.97	0.07	0.06
KH-12-4, BD17, 132.40°W, 43.00°N, depth 3732 m, 27−28 September 2012								
11	0.41	1.20			0.41	1.20		
25	0.53	1.00			0.53	1.00		
50	0.48	0.98			0.48	0.98		
55	0.47	1.16			0.47	1.16		
99	0.54	1.29			0.54	1.29		
199	0.53	0.98			0.53	0.98		
396	0.62	1.59			0.62	1.59		
792	0.85	1.64			0.85	1.64		
989	0.78	1.75			0.78	1.75		
1975	0.74	2.74			0.74	2.74		
2466	0.80	2.84			0.80	2.84		
2956	0.76	3.17			0.76	3.17		
3445	0.66	3.57			0.66	3.57		
3695	0.66	4.24			0.66	4.24		

Supplementary Table 1 (continued)

Depth [m]	First analysis		Second analysis		Average		2 s.d.	
	$\delta^{65}Cu$ [‰]	Cu [nmol kg^{-1}]	$\delta^{65}Cu$ [‰]	Cu [nmol kg^{-1}]	$\delta^{65}Cu$ [‰]	Cu [nmol kg^{-1}]	$\delta^{65}Cu$ [‰]	Cu [nmol kg^{-1}]
KH-12-4, BD21, 128.43°W, 48.45°N, depth 2438 m, 30 September−1 October								
11	0.44	2.09			0.44	2.09		
100	0.59	1.36			0.59	1.36		
298	0.66	1.71			0.66	1.71		
594	0.68	1.89			0.68	1.89		
1186	0.78	2.06			0.78	2.06		
1777	0.75	2.63			0.75	2.63		
1974	0.74	2.94			0.74	2.94		
2071	0.74	2.96			0.74	2.96		
2170	0.71	2.97			0.71	2.97		
2268	0.70	2.60			0.70	2.60		
2366	0.71	3.17			0.71	3.17		
2399	0.69	3.06			0.69	3.06		

Supplementary Table 1 (continued)

Depth [m]	First analysis		Second analysis		Average		2 s.d.	
	$\delta^{65}Cu$ [‰]	Cu [nmol kg^{-1}]	$\delta^{65}Cu$ [‰]	Cu [nmol kg^{-1}]	$\delta^{65}Cu$ [‰]	Cu [nmol kg^{-1}]	$\delta^{65}Cu$ [‰]	Cu [nmol kg^{-1}]
KH-09-5, ER10, 72.55°E , 20.00°S , depth 4343 m, 11 December 2009								
11	0.48	1.13	0.48	1.14	0.48	1.13	0.01	0.02
25	0.51	1.07	0.52	1.09	0.52	1.08	0.02	0.03
51	0.50	1.01	0.46	1.01	0.48	1.01	0.05	0.01
99	0.50	0.90	0.55	0.90	0.53	0.90	0.07	0.01
150	0.58	0.90	0.55	0.89	0.57	0.90	0.05	0.01
199	0.61	0.79	0.57	0.77	0.59	0.78	0.06	0.02
400	0.61	0.78			0.61	0.78		
597	0.63	0.81			0.63	0.81		
795	0.59	1.25			0.59	1.25		
993	0.64	1.60			0.64	1.60		
1240	0.66	1.70			0.66	1.70		
1486	0.69	1.86			0.69	1.86		
1979	0.70	2.45			0.70	2.45		
2470	0.65	2.81			0.65	2.81		
2962	0.62	3.15			0.62	3.15		
3452	0.60	3.68			0.60	3.68		
3941	0.63	3.76			0.63	3.76		
4306	0.63	3.85			0.63	3.85		
BATS, 64.10°E, 31.40°N, depth 4500 m								
2000	0.41	1.70			0.41	1.59		
D357, #163, 13.39°E , 36.46°S, depth 4894 m								
4723	0.44	2.87	0.42	2.89	0.43	2.88	0.03	0.01
				Average	0.60	2.20	0.045	0.11
				n	77	77	34	34

Supplementary Table 2 Box model for Cu cycling in the ocean[a]

			δ^{65}Cu	Cu flux [10^9 mol y^{-1}]
Surface seawater	Input	Atmospheric	0.00	0.96
		Riverine	0.68	0.76
[Cu] = 1.1 nmol kg^{-1}		Upwelling	0.60	3.0
δ^{65}Cu = 0.49	Output	Downwelling	0.49	1.3
		Particulate	0.49	3.4
Deep seawater	Input	Downwelling	0.49	1.3
		Benthic	0.58	3.7
[Cu] = 2.5 nmol kg^{-1}		Particulate	0.49	3.4
δ^{65}Cu = 0.60	Output	Upwelling	0.60	3.0
		Particulate	0.49	5.4
Scavenged Layer	Input	Particulate	0.49	5.4
	Output	Benthic	0.58	3.7
		Preserved	0.30	1.7

[a] Black and magenta figures are the observed and calculated values, respectively.

Supplementary Methods

Intercalibration of seawater $\delta^{65}Cu$

We performed the intercalibration of $\delta^{65}Cu$ with the ETH group using a seawater sample collected at a depth of 7145 m near the Japan Trench (TR17, 143.87°E, 37.81°N, bottom depth 7150 m). This sample was divided into 4 aliquots and analysed twice with both the methodology of the ETH group and our method. The obtained $\delta^{65}Cu$ values were consistent between the ETH group and us, as shown in Supplementary Fig. 4.

The ETH group pre-concentrated Cu from seawater using a co-precipitation technique with $Al(OH)_3$. The detail of this technique is described in Zhao et al. (2014)[6]. The pre-concentrated metal fraction was purified twice using anion exchange chromatography, as described in Archer and Vance (2004)[7]. The purified sample was oxidised by refluxing in HNO_3+H_2O_2 (ref. 8). After evaporating the sample to dryness, the residue was re-dissolved with 2% nitric acid for isotopic measurements on a multi-collector ICP-MS. The setting of the multi-collector ICP-MS is detailed in Little et al. (2014)[8].

Supplementary References

1. Vu HTD & Sohrin Y. Diverse stoichiometry of dissolved trace metals in the Indian Ocean. *Sci. Rep.* **3**, 1745 (2013).

2. Bermin J, Vance D, Archer C & Statham PJ. The determination of the isotopic composition of Cu and Zn in seawater. *Chem. Geol.* **226**, 280-297 (2006).

3. Vance D, *et al.* The copper isotope geochemistry of rivers and the oceans. *Earth Planet. Sci. Lett.* **274**, 204-213 (2008).

4. Boyle EA, *et al.* GEOTRACES IC1 (BATS) contamination-prone trace element isotopes Cd, Fe, Pb, Zn, Cu, and Mo intercalibration. *Limnol. Oceanogr, Methods* **10**, 653-665 (2012).

5. Thompson CM, Ellwood MJ & Wille M. A solvent extraction technique for the isotopic measurement of dissolved copper in seawater. *Anal. Chim. Acta* **775**, 106-113 (2013).

6. Zhao Y, Vance D, Abouchami W & de Baar HJW. Biogeochemical cycling of zinc and its isotopes in the Southern Ocean. *Geochim. Cosmochim. Acta* **125**, 653-672 (2014).

7. Archer C & Vance D. Mass discrimination correction in multiple-collector plasma source mass spectrometry: An example using Cu and Zn isotopes. *J. Anal. At. Spectrom.* **19**, 656-665 (2004).

8. Little SH, Vance D, Walker-Brown C & Landing WM. The oceanic mass balance of copper and zinc isotopes, investigated by analysis of their inputs, and outputs to ferromanganese oxide sediments. *Geochim. Cosmochim. Acta* **125**, 673-693 (2014).